



Research papers

Increase in probable maximum precipitation in a changing climate over India

Subharthi Sarkar, Rajib Maity*

Department of Civil Engineering, Indian Institute of Technology Kharagpur, Kharagpur 721302, West Bengal, India

ARTICLE INFO

Keywords:

Annual maximum daily precipitation (AMDP)
 Modified Hershfield method
 Enveloping technique
 Frequency factor
 Climate change
 Change in PMP

ABSTRACT

Probable Maximum Precipitation (PMP) is considered as an important design criteria and it is expected to change over time owing to the impacts of climate change and intensification of global hydrological cycle. Thus, reconstruction of PMP map and investigation about its temporal change are very essential in the context of climate change. This study develops 1-day PMP map of India for five consecutive time periods (two in historical, i.e., 1901–70, 1971–2010; and three in future, i.e., 2010–39, 2040–69 and 2070–2100) to study its temporal change. Observed gridded daily precipitation data from India Meteorological Department (IMD) and outputs from three climate models following two Representative Concentration Pathways (RCPs) are used to develop historical and future PMP maps, respectively. The modified Hershfield method is used for estimation of PMP with an updated method for enveloping technique. The results show a clear increasing trend in PMP for most part of India. Specifically, 84% area of Indian mainland exhibits an increasing trend in PMP with an average of around 35% increase in post-1970 (1971–2010) period as compared to pre-1970 (1901–1970) period. Similarly, in the far-future period (2071–2100), around 70–80% area is showing an increase with an approximate average increase of 20%–35% in PMP across different models with respect to recent past (1971–2010) following RCP 8.5 scenario. These observations evidently indicate how significantly PMP is increasing due to climate change and it should be considered in the revised planning and design in water resources engineering.

1. Introduction

Intensification of hydrological cycle is one of the major consequences of climate change (Jacob and Hagemann, 2007; Allen and Ingram, 2002). Such intensification leads to higher intensity and frequency of precipitation events at global and local scale (Trenberth et al., 2003; Giorgi et al., 2011). Increase in extreme precipitation is being reported in many studies (Allan and Soden, 2008; Utsumi et al., 2011; O’Gorman, 2015; Madakumbura et al., 2019). As a consequence of such intensification, Probable Maximum Precipitation (PMP), which is defined as “the greatest depth of precipitation for a given duration that is physically possible over a given size storm area at a particular geographical location at a certain time of year” (WMO, 1986), is expected to increase with time. The usefulness of PMP in hydrologic studies and design ranges from estimation of Probable Maximum Flood (PMF) (Fernando and Wickramasuriya, 2011) to the design of major hydraulic structures such as large dams (WMO, 2009) to the design of high-risk energy infrastructures like nuclear power plants (Prasad et al., 2011). The possible change in PMP will have some serious implications on such structures due to their very long life span (>100–500 years) and may

alter the risk and reliability associated with such structures, designed against a stationary estimate of PMP (Kunkel et al. 2013; Milly et al., 2008). Hence, the study on temporal change of PMP is of utmost importance in the context of climate change, which is the focus of this study.

Possible impact of climate change on the PMP has been reported in the literature at different parts of the world. For instance, Kunkel et al. (2013) showed that the PMP is likely to increase in future as indicated by simulation results of various Global Circulation Models (GCMs) due to substantial increase in average and maximum atmospheric moisture content. Analysing the downscaled climatic projections produced by the Canadian Regional Climate Model (CRCM), Beauchamp et al. (2013), and Rouhani and Leconte (2016) indicated a tendency of increasing PMP estimates over different watersheds in Quebec. Rastogi et al. (2017) projected a significant increase in PMP estimates in later part of 21st century over the Alabama-Coosa-Tallapoosa (ACT) River Basin in the south-eastern United States, using a physics-based numerical weather simulation model. Stratz and Hossain (2014) studied on non-stationary PMP recalculations at three large dam sites in the United States and reported a substantial increase in currently accepted PMP

* Corresponding author.

E-mail address: rajib@civil.iitkgp.ac.in (R. Maity).

values under future climate changes. [Chen et al. \(2017\)](#) also reported an increase in PMP in the Pacific Northwest (PNW) region in the USA by about $50\% \pm 30\%$ around 2099 relative to the 2016 level, under the worst climate scenario (RCP8.5). Likewise, many studies have investigated the impact of climate change on PMP and reported a general increasing trend in future around different parts of the world ([Rousseau et al. 2014](#); [Afrooz et al., 2015](#); [Klein et al., 2016](#); [Lee et al., 2016](#); [Ramak et al., 2017](#); [Thuy et al., 2019](#)). However, none of these studies investigated the effect of shift in global climatic regime in 1970s ([Wang et al., 2001](#); [Zhou et al., 2009](#); [Sabeerali et al., 2012](#); [Chen et al., 2007](#); [Dai et al., 2018](#); [Dash and Maity, 2019](#)) on PMP. This shift in climatic regime, caused by anthropogenic global warming and different other external forcings, is found to have significant impacts on several important hydroclimatic variables, such as temperature, air pressure, wind field, and rainfall pattern ([Wang, 2001](#); [Meehl et al., 2008](#); [Jacques-coper and Garreaud, 2015](#)). Nevertheless its effect on precipitation extremes especially on PMP is yet to be explored, which motivates the present study to investigate the impact of shift in global climatic regime in 1970s on the spatio-temporal variation of PMP, considering the entire Indian mainland as the study area. Secondly, though there have been several works conducted at different regions/basins in India to estimate PMP by different methods ([Mazumder and Rangarajan, 1966](#), [Sharma et al., 1975](#); [Dhar et al., 1981](#); [Rakhecha et al., 1992](#); [Kulkarni, 2000](#); [Chavan and Srinivas, 2017](#)), no significant work on future changes in PMP is available. Currently, India has 5264 completed large dams and 437 large dams are under construction (Available on <http://www.indiaenvironmentportal.org.in/files/file/NRLD%202018.pdf> accessed in June 2019). These dams will experience future changes in climate owing to their long life spans. These two factors build the motivations of this study, i.e., to investigate the impact of climate change on the spatio-temporal variation of PMP in the past (to study the impact of global climate regime shift in 1970s) and in the future (which can be useful for future risk assessment of existing hydrologic structures) in India.

Among many methods available in literature (e.g., [Wiesner, 1970](#); [Hansen et al., 1977](#); [Schreiner and Riedel, 1978](#); [Hart, 1981](#); [Collier and Hardaker, 1996](#)), Hershfield method ([Hershfield, 1961, 1965](#)) is considered as a convenient and efficient tool for the estimation of PMP, particularly for those locations where sufficiently long precipitation records are available but other meteorological data (e.g., dew point temperature, wind speed, relative and humidity) are lacking. These meteorological data are essential for other physical methods, such as moisture maximization and storm transposition technique ([WMO, 2009](#); [Singh et al., 2018](#)). With the availability of sufficiently long record of precipitation, the PMP estimates by Hershfield method are closely comparable to those by other approaches at different parts of the world, e.g., [Bruce and Clark \(1966\)](#) for Canada, [Myers \(1967\)](#) for the USA, [Eliasson \(1997\)](#) for Iceland and [Wiesner \(1970\)](#) for Australia. The World Meteorological Organisation (WMO) has also recommended the Hershfield method as one of the methods to estimate PMP in their various manuals and technical publications ([WMO, 2009](#)). Considering its benefits, the [Hershfield \(1965\)](#) method is used for estimating PMP in this study, however, with a modified enveloping technique, discussed elaborately later.

In brief, the overall objective of this study is to investigate the

possible spatio-temporal change in PMP over India under changing climate. To capture this change in PMP, 1-day PMP maps are developed for the entire Indian mainland for five consecutive time periods, spanning over 200 years from past to future – two historical periods, viz. pre-1970 (1901–1970) and post-1970 (1971–2010) and three future time periods, viz. near-future (2011–2040), future (2041–2070) and far-future (2071–2100), following two possible climate change scenarios (RCP 4.5 and RCP 8.5). These PMP maps, especially the recent one (post-1970) and its future projections will serve as an important information for the design engineers and hydro-meteorologists for revised planning and designing various major water-energy infrastructures in the context of climate change. The remaining part of this paper is organized as follows.

Details on the observed and future simulated rainfall data are provided in section 2. Following this, the methodology, along with the proposed modification in the standard enveloping technique for estimation of PMP using Hershfield method (1965), is explained in section 3. Results in terms of PMP maps in the past and future time periods are presented in [Section 4](#) along with associated comparative study. Finally, the conclusions of the study are provided in [Section 5](#).

2. Rainfall data used

2.1. Historical observed data from IMD

Daily gridded (0.25° latitude \times 0.25° longitude) rainfall data over entire Indian mainland is procured from India Meteorological Department (IMD). The length of the data is 110 years, i.e., from 1901 to 2010. It is split into two parts, pre-1970 (1901–1970) and post-1970 (1971–2010), to capture the effect of the shift in global climate regime in the 1970s as mentioned before. Though it is not an equal division of the historical data, the data lengths are sufficiently long for both pre- and post-1970 periods to estimate PMP.

Next, 1-day annual maximum rainfall values are extracted and the series of Annual Maximum Daily Precipitation (AMDP) values are prepared at each grid point. As an initial checking, it is noticed that at some grid points in the north-east region, the recorded rainfall magnitude is zero throughout the year for many consecutive years. It may be due to non-availability of data in these regions. This is particularly true for the pre-1970 period. Such cases are ignored from the analysis.

2.2. Future RCM data from CORDEX

Coordinated Regional Downscaling Experiment (CORDEX) portal, supported by World Climate Research Programme (WCRP), provides the simulation outputs of various climate variables during historical and future time periods at a regional scale ([Nikulin et al., 2011](#)). In this study, daily simulated precipitation values for the future time period 2011–2100 (i.e., 90 years) are obtained for three different Regional Climate Models (RCMs), for two emission scenarios, designated by Representative Concentration Pathways (RCP 4.5 and RCP 8.5) from the CORDEX database. The basic information of the data, including its driving model, source institute, data resolution for those three different model-combinations (named as M1, M2, and M3 henceforth) are shown in [Table 1](#). Similar to historical data, the length of future simulated data

Table 1
Details of future simulated precipitation data used in this study.

Model Abbreviation	Driving GCM	Source Institute	Used scenarios	RCM	Data resolution
M1	MPI-ESM-LR	Max Planck Institute for Meteorology	RCP 4.5 RCP 8.5	MPI-CSC-REMO2009	$0.5^\circ \times 0.5^\circ$
M2	CCCma-CanESM2	Swedish Meteorological and Hydrological Institute	RCP 4.5 RCP 8.5	SMHI-RCA4	$0.44^\circ \times 0.44^\circ$
M3	MOHC-HadGEM2	same	RCP 4.5 RCP 8.5	SMHI-RCA4	$0.44^\circ \times 0.44^\circ$

i.e., 90 years is also divided into three equal parts of 30 years, namely near-future (2011–40), future (2041–70), and far-future (2071–2100) to study the change in PMP estimates over time. However, to use any future climate model output, bias with respect to observed data is to be corrected. For the bias correction, historically simulated daily precipitation values for the concerned climate model are required. Hence, along with future data, historical data (1961–2005) are also obtained for M1, M2, and M3.

3. Methodology

Initially, the daily observed rainfall data undergone some preliminary screening, including removal of spurious data (e.g., zero rainfall years, as discussed in section 2.1). As explained earlier, any simulated climate model output (here RCM output) may possess significant bias with respect to actual observations, in spite of some recent developments in the field (Jang and Kavvas, 2015). Hence, the selection of a suitable bias correction method and application of that on the future simulated rainfall data is a mandatory step in the analysis. Next, the homogeneity of both observed and future AMDP series at each grid point is checked by the Mann Kendall test followed by adjustment of mean and standard deviation for the sample size and observed maximum event. Finally, the estimation of PMP as per the modified Hershfield method starts with the evaluation of frequency factor and its upper envelope curve. Finally, a comparative study is carried out between developed PMP maps for the future time periods and recent past to capture the temporal change of PMP. The entire methodology starting from data collection to final comparative study is summarised in Fig. 1 in the form of a flowchart. Major steps involved in the methodology are discussed in the subsequent sections.

3.1. Bias correction for future-simulated precipitation series

Most of the existing bias-correction techniques correct the bias in mean values only, not in extreme values. However, as the present study involves only annual maximum values, a bias-correction method for extreme values is required. Also, in case of monsoon-dominant country like India, consideration of zero-rainfall days in the calculation plays a key role in bias correction, what most of the bias correction methods ignore (Maity et al., 2019). Hence, a recently developed copula-based bias-correction technique, developed by Maity et al. (2019), is used. This method is proven to correct the bias in both mean and extreme values, and suitable for zero-inflated daily simulated precipitation series. The method uses copula (Nelsen, 2006; Maity, 2018) to develop the joint distribution between observed and simulated precipitation in the past over a particular time period. Then, the conditional distribution function obtained from the joint distribution is modified as a mixed distribution with a discrete probability mass at zero in order to account for zero values. Finally, using the future-simulated precipitation values as input into the modified conditional distribution function, future bias-corrected values are simulated and used for subsequent steps for PMP estimation.

3.2. Checking the homogeneity of data series

The use of a long series of annual maximum daily rainfall in the estimation of PMP is suitable only if they show no significant increasing or decreasing trends (Desa and Rakhecha, 2007). The presence or absence of trends in the annual maximum rainfall series can be investigated using the Mann–Kendall rank statistics test (WMO, 1966), or Swed-Eisenhart run test (WMO, 1966), or turning point test (Kendall and Stuart, 1976). The Mann–Kendall rank statistics test is used and the test statistic (τ) is defined as

$$\tau = \frac{4 \sum n_i}{N(N-1)} - 1 \quad (1)$$

where n_i is the number of values larger than the i^{th} value in the series subsequent to its position in the series of N values. This statistic (τ) follows a normal distribution with its expected value zero and variance given by Eq. (2).

$$\sigma_\tau^2 = \frac{4N + 10}{9N(N-1)} \quad (2)$$

So, the standardised variate of τ , i.e. the ratio of τ to the σ_τ , gives an indication of trend in the data. For no trend in the data series, this value should lie within the limits of ± 1.96 at the 5% level of significance and within the limits of ± 2.576 at the 1% level of significance.

3.3. Adjustment of mean and standard deviation for the maximum event

Extreme rainfall amounts of rare magnitude (e.g. rainfall with return periods of 500 years or more) are generally considered as an outlier in any data series. Though these outliers are not ignored from the analysis, these values may have some substantial effect on the mean and standard deviation of the data series. The magnitude of this effect is less for long records of data than for short records. Hershfield (1961) studied this by using hypothetical series of varying length and developed Mean Adjustment Factor (MAF_1) and Standard deviation Adjustment Factor (SAF_1) for different data lengths. The adjustment factors (MAF_1 and SAF_1) need to be multiplied with the originally calculated mean and standard deviation to obtain their corresponding adjusted values for each grid point. It must be noted that this adjustment considers only the effect of the maximum observed event, not other anomalous observations (WMO, 1986).

3.4. Adjustment of mean and standard deviation for sample size

In general, the frequency distribution of extreme rainfall is skewed towards right, and hence, there is always a greater chance of getting a large extreme event than a smaller extreme with the increase in the length of record (WMO, 2009). As a result of that, the mean and standard deviation of the annual maximum series tend to increase with the length of record. Hence, Hershfield (1961) proposed another set of adjustment factors for mean (MAF_2) and standard deviation (SAF_2) for different sample sizes. In our study, we have evaluated the adjusted values of mean and standard deviation after incorporating these both sets of adjustment factors.

$$\bar{X}_N = \tilde{X}_N \times MAF_1 \times MAF_2 \quad (3)$$

$$\bar{S}_N = \tilde{S}_N \times SAF_1 \times SAF_2 \quad (4)$$

where \tilde{X}_N and \tilde{S}_N are the original mean and standard deviation of the annual maximum time series, respectively; N is the number of years of data; \bar{X}_N and \bar{S}_N are the adjusted mean and standard deviation of data series, respectively.

3.5. Basic equations in Hershfield method

Hershfield (1961) proposed the basic equation for estimation of PMP based on the general frequency equation suggested by Chow (1951), as follows:

$$X_{PMP} = \bar{X}_N + K \times \bar{S}_N \quad (5)$$

where X_{PMP} is the PMP estimate for the station, \bar{X}_N is the adjusted mean of the annual maximum series of rainfall data for N years at that station, \bar{S}_N is the adjusted standard deviation of the annual maximum series of rainfall data at that station, K is the frequency factor for estimating PMP at that station, which can be determined from the following equation, proposed by Hershfield (1961),

$$K = \frac{X_m - \tilde{X}_{N-1}}{\tilde{S}_{N-1}} \quad (6)$$

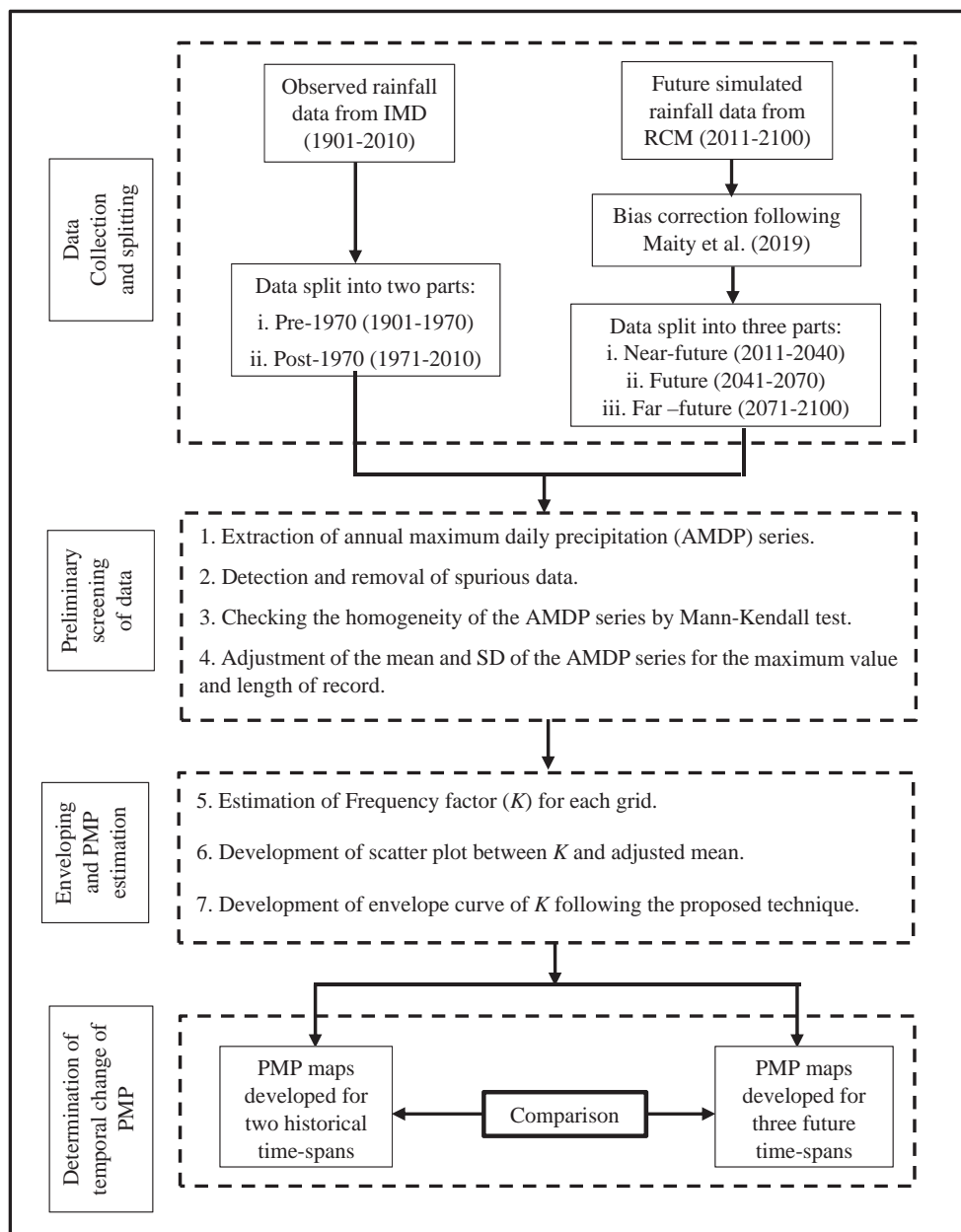


Fig. 1. Methodological flowchart of PMP estimation in this study.

where X_m is the maximum value in annual maximum series of rainfall data at the station, \bar{X}_{N-1} and \bar{S}_{N-1} are the mean and standard deviation of the annual maximum series of rainfall data, respectively for $(N-1)$ years after removing the year with the maximum value.

3.6. Development of upper envelope curve of frequency factor

Judicious estimation of frequency factor K plays a key role in proper estimation of PMP. A very high value of K will lead to over-estimation of PMP and consequently an uneconomical design. On the other hand, a lower value of K will lead to under-estimation of PMP and any structure designed based on that PMP estimate will be exposed to higher risk. So, the factor K has to be determined appropriately such that the design based on it, have a proper balance of economy and allowable risk.

For this purpose, the upper envelope curve of K is used as proposed by Hershfield (1965). From the simple scatter plot between K and \bar{X}_N for 2700 stations (90% in the USA) across the globe, Hershfield (1965) found a general, negative trend in the plot, i.e. as \bar{X}_N increases, K

decreases. Depending on that, one exponential function of K is developed for different duration of rainfall as its upper envelope curve, as given below.

$$K = K_A e^{-a\bar{X}_N} \quad (7)$$

As per the Eq. (7), the envelope curve starts at some point K_A in the K axis (for $\bar{X}_N = 0$) and exponentially decreases and becomes asymptotic towards the higher values of \bar{X}_N . Hershfield (1965) used 20 as the value of K_A after analysing data from 2700 different locations as mentioned earlier, but this value may vary for different study areas. The slope of the exponentially decreasing curve depends on the factor 'a', which is again a function of study area and duration of the rainfall. However, in this technique, it is noticed that unusually high values may be assigned to the points with lower mean due to the steep nature of the exponential curve towards the left end. A typical example of scatter plot is shown in Fig. 2, where some points on the possible upper envelope are selected (shown by orange diamond dots), and an exponential curve (blue dashed line) is fitted to those points. This blue dashed exponential

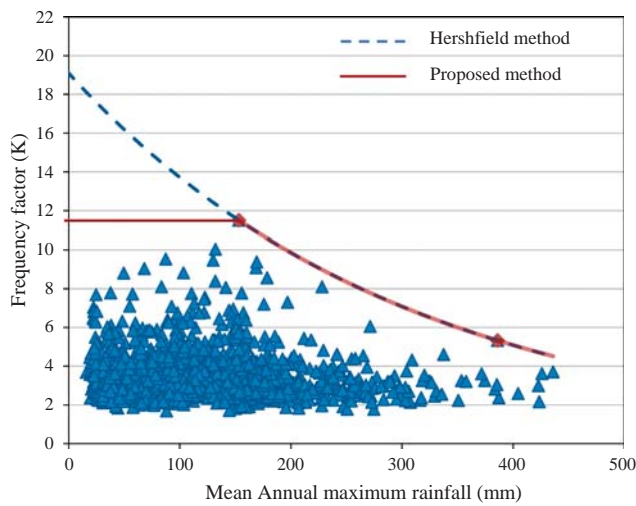


Fig. 2. A typical upper envelope curve for Frequency Factor according to Hershfield (1965) and the proposed method in this study.

curve indicates the envelope curve following Hershfield (1965). Though the maximum value of K (say K_m) is 11.5 here, the envelope curve meets the K -axis around 19 and thus provides excessive weightage (more than the maximum value of K in the study area) to the points with lower mean AMDP magnitude. This may not be a realistic reflection of the data points and thus leading to overestimation of PMP in those low-precipitation extreme region. Hence, a modified technique of enveloping is introduced in this study ensuring that no grid point gets assigned with $K > K_m$ within the study area. In this modified enveloping technique, instead of a single envelope curve (as in the existing Hershfield method), a composite envelope curve is proposed comprising of a straight line (parallel to x -axis) part and an exponentially decay curve, same as the blue dashed line. Thus, the revised envelope curve not only encapsulates all the observed frequency factors, but also unusually high values are avoided for the low rainfall regions. A typical

example of such modified envelope curve is shown as the red line in Fig. 2, from which it can be seen that the straight line portion and the exponential curve intersects at mean AMDP (\bar{X}_N) = \bar{X}_N^t (t refers to transition point) and frequency factor (K) = K_m , where \bar{X}_N^t denotes the mean AMDP at transition point and K_m is the highest value of K . Thus, the revised curve is defined by Eq. (8) as follows:

$$K = \begin{cases} K_m & 0 < \bar{X}_N \leq \bar{X}_N^t \\ K_m e^{-b(\bar{X}_N - \bar{X}_N^t)} & \bar{X}_N > \bar{X}_N^t \end{cases} \quad (8)$$

In this revised envelope curve also, a factor ‘ b ’ is there, which determines the slope of the exponentially decreasing portion, and is a function of the duration of interest and the study area. Referring to Fig. 2, the revised envelope curve consists of a straight line $K = K_m$ ($= 11.5$, here) for the mean AMDP zero to \bar{X}_N^t ($= 153$ mm, here) and an exponentially decaying curve for mean AMDP higher than 153 mm. Finally, using the new values of frequency factor from the envelope curve, PMP at any location can be estimated using Eq. (5).

3.7. Determination of change in PMP over time

In order to identify the impact of global shift in climate regime in the 1970s on PMP, the PMP map for post-1970 is compared with that of pre-1970 in terms of percentage difference. Likewise, to capture the change in future PMP estimates over time, PMP maps developed for three future time spans for three models and two scenarios are compared with the recent past, i.e., post-1970 PMP values at each grid point. Plotting this percentage change in PMP will provide the spatial distribution of this change throughout India. However, due to mismatch in the data resolution between observed (here, $0.25^\circ \times 0.25^\circ$) and future ($0.5^\circ \times 0.5^\circ$ or $0.44^\circ \times 0.44^\circ$) period, observed data is re-gridded by Inverse Distance Weightage (IDW) method to match the corresponding future data for calculating the percentage change in PMP in future with respect to recent past. IDW method is a widely used interpolation technique in hydro-meteorological studies (Tang et al., 1996; Xia et al., 1999; De Silva et al., 2007; Chen and Liu, 2012), which determines the value of a variable at a target location through a linear combination of

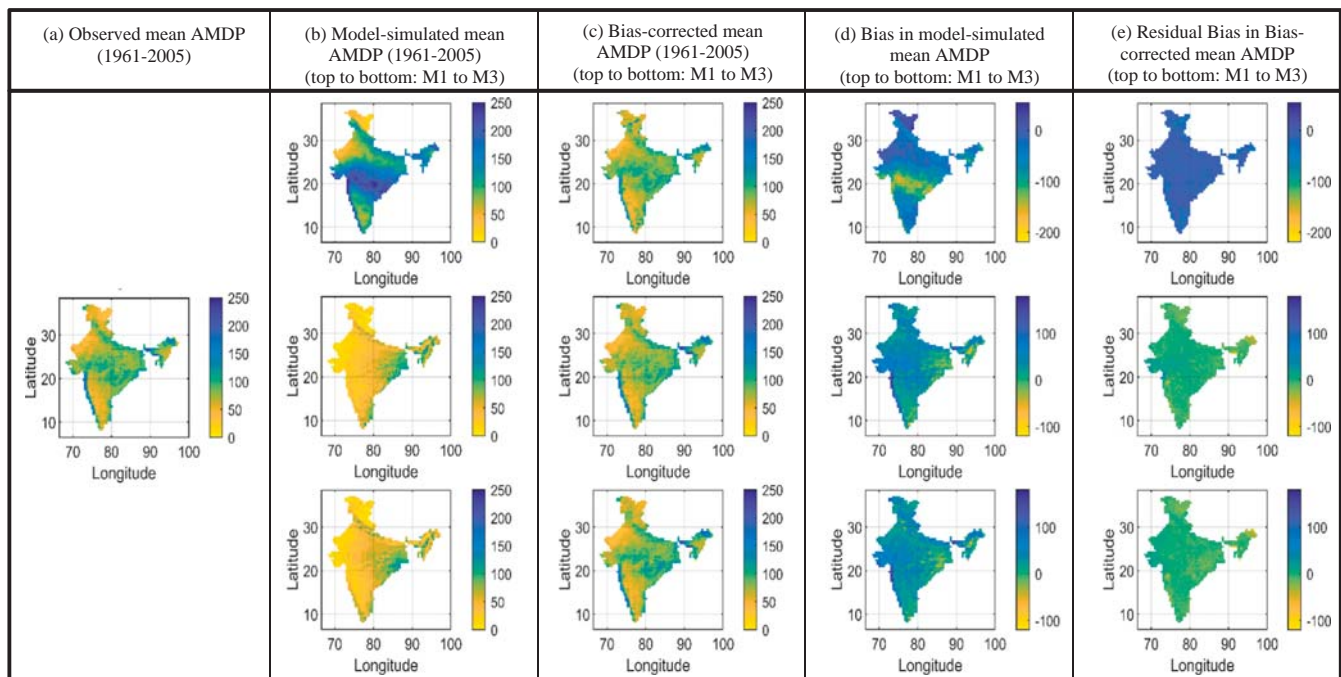


Fig. 3. Results of Bias correction (as per Maity et. al, 2019) for mean AMDP, used in this study, (a) Observed mean AMDP (1961–2005), (b) Model-simulated mean AMDP (1961–2005), (c) Bias-corrected mean AMDP (1961–2005), (d) Bias in the model-simulated mean AMDP, and (e) Residual Bias in Bias-corrected mean AMDP, for M1, M2, and M3 (top to bottom), respectively.

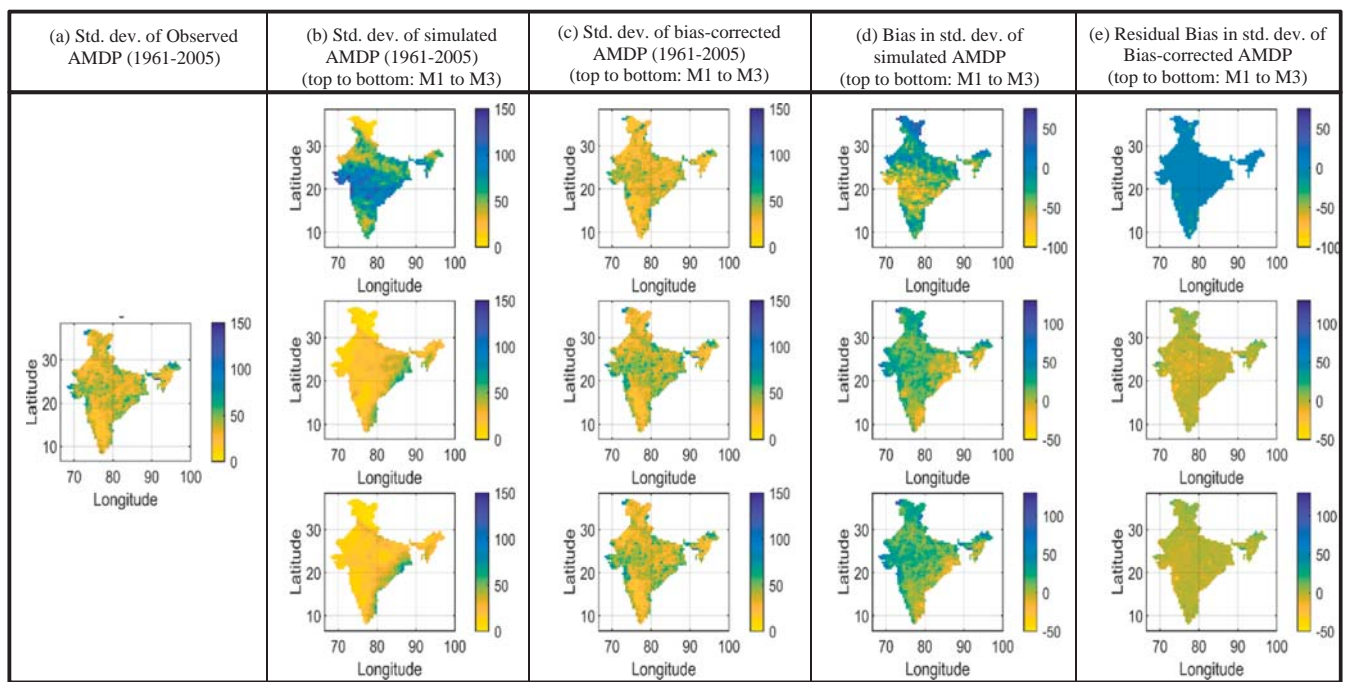


Fig. 4. Results of Bias correction (as per Maity et. al, 2019) for standard deviation of AMDP, used in this study, (a) Std. dev. of observed mean AMDP (1961–2005), (b) Std. dev. of model-simulated mean AMDP (1961–2005), (c) Std. dev. of bias-corrected mean AMDP (1961–2005), (d) Bias in the std. dev. of model-simulated AMDP, and (e) Residual Bias in the std. dev. of bias-corrected mean AMDP, for M1, M2, and M3 (top to bottom), respectively.

Table 2a

Results of Mann-Kendall rank test for observed precipitation series.

Different cases	Percentage of grid-points showing no significant trend	
	(5% significance level)	(1% significance level)
Pre-1970 period (1901–1970)	80.32	89.59
Post-1970 period (1971–2010)	85.07	94.22

Table 2b

Results of Mann-Kendall rank test for future-simulated precipitation series: percentage of grid points showing no significant trend.

Model	Scenario	Near future (2011–2040)		Future (2041–2070)		Far-future (2071–2100)	
		5% level	1% level	5% level	1% level	5% level	1% level
M1	RCP 4.5	95.58	99.54	96.59	99.45	93.74	99.17
	RCP 8.5	94.29	98.89	90.61	97.79	94.11	99.08
M2	RCP 4.5	93.44	98.22	94.48	98.69	96.26	99.41
	RCP 8.5	95.60	99.35	95.73	99.21	95.34	98.62
M3	RCP 4.5	94.29	99.02	94.09	98.56	95.41	99.34
	RCP 8.5	95.80	99.41	95.34	99.48	94.42	98.56

the values at four surrounding grid intersections, by assigning weights inversely proportional to the distance from the target location to the grid intersections.

4. Results and discussion

4.1. Results of bias correction

Before applying any bias correction technique, a comparative study has been conducted between the observed and model-simulated (from

M1, M2, and M3) precipitation series over a common historical period (1961–2005). The results reveal the presence of significant bias in the mean and standard deviation of the extreme values (i.e., AMDP here) of model-simulated precipitation series with respect to that of observed. The mean values of AMDP from observed records and outputs from three different models are shown in first two panels of Fig. 3 (a and b), respectively. Inter-model spatial variations are notable and the existence of bias in the model-simulated (from M1, M2, and M3) precipitation values is shown in panel ‘d’ of Fig. 3. It shows that the model M1 possesses a considerable amount of negative bias (i.e. simulated values are higher than observed) in mean AMDP along the central belt of India, whereas the models M2 and M3 have huge positive bias (i.e. observed values are higher than simulated) in the western and some parts of north-east India. Apart from mean, standard deviation of AMDP series are also compared (Fig. 4). Similar observations are made from Fig. 4 as well, which illustrates the difference in the standard deviation between observed and simulated AMDP series all over India, across the models.

As discussed in section 3.1, a recently developed copula-based bias-correction technique (Maity et al., 2019) is used to remove this bias present in the extreme values. Bias corrected results in terms of mean and standard deviation of AMDP (1961–2005) are presented in panel ‘c’ of Figs. 3 and 4, respectively. The plots showing the residual bias are also presented in panel ‘e’ of Figs. 3 and 4. The residual bias is approximately near-zero throughout the Indian mainland. Comparing the figures in panel ‘e’ with those in panel ‘d’, it is noticed that the bias-correction method, adopted in this study, has effectively debiased the model-simulated precipitation in terms of both mean and standard deviation of the AMDP series. Using the same bias-correction technique, future-simulated daily precipitation series are also bias-corrected.

4.2. Mann Kendall rank statistic test for detection of trend

Tables 2a and 2b show the results of the Mann-Kendall test for observed and future-simulated AMDP series, respectively at two levels of significance, i.e., 5% and 1%. These results depict that most part of India is not showing any significant trend in AMDP series, and hence,

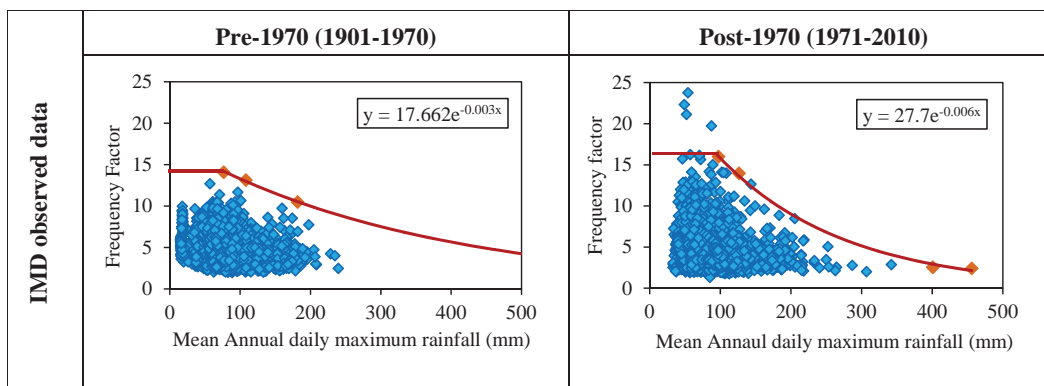


Fig. 5a. Scatter plot and upper envelope curve of frequency factor for two parts of IMD observed data, viz. pre-1970 and post-1970. The orange dots show the points used to develop the envelope curve. The equation of the exponential position of the envelope curve is given in inset. (For interpretation of the references to colour in this figure legend, the reader is referred to the web version of this article.)

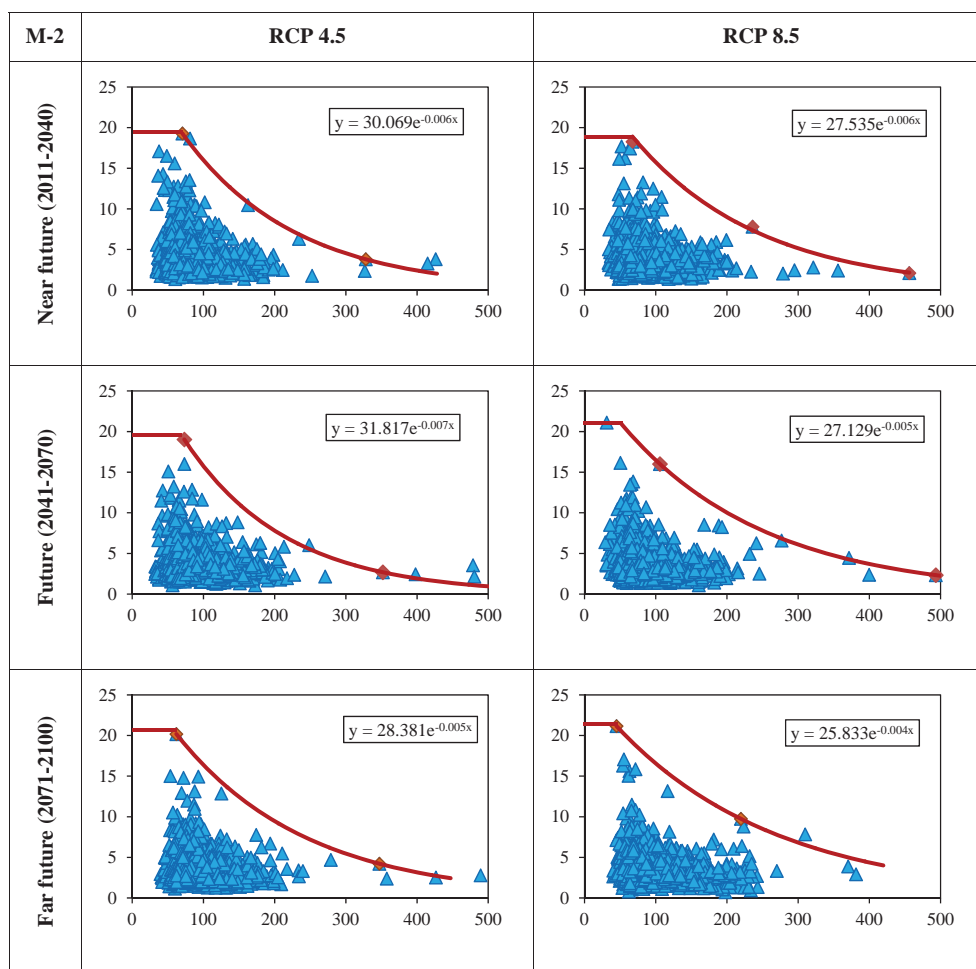


Fig. 5b. As in Fig. 5a but for three future time periods, following RCP 4.5 and RCP 8.5 scenario for M2 (as a representative sample). The X-axis represents mean annual maximum precipitation (mm) and Y-axis represents frequency factor (K) in all subplots.

this time series can safely be considered as homogeneous for entire India in subsequent calculations.

4.3. Determination of frequency factor and its envelope curve

Using Eq. (6), frequency factor K is determined for each grid point throughout India for different time-spans and models. Scatter plot of K against mean annual maximum daily rainfall (\bar{X}_N) for two parts of observed data is shown in Fig. 5a and the same is shown for three

of future data for M2 following RCP 4.5 and RCP 8.5 in Fig. 5b (for brevity, results for M1 and M3 are not shown by figure). From these scatter plots, a general trend of decreasing K with increasing \bar{X}_N is observed. Moreover, it is noticed that the K values are highly skewed towards its lower side. In other words, the K value falls within a small range of 2–10 for most of the grid points. These observations match with the findings of other investigators (Desa and Rakhecha, 2007; Rakhecha et al., 1992; Kim and Lee, 2016; Hershfield, 1965). For each scatter plot, the upper envelope curve for K is developed by applying

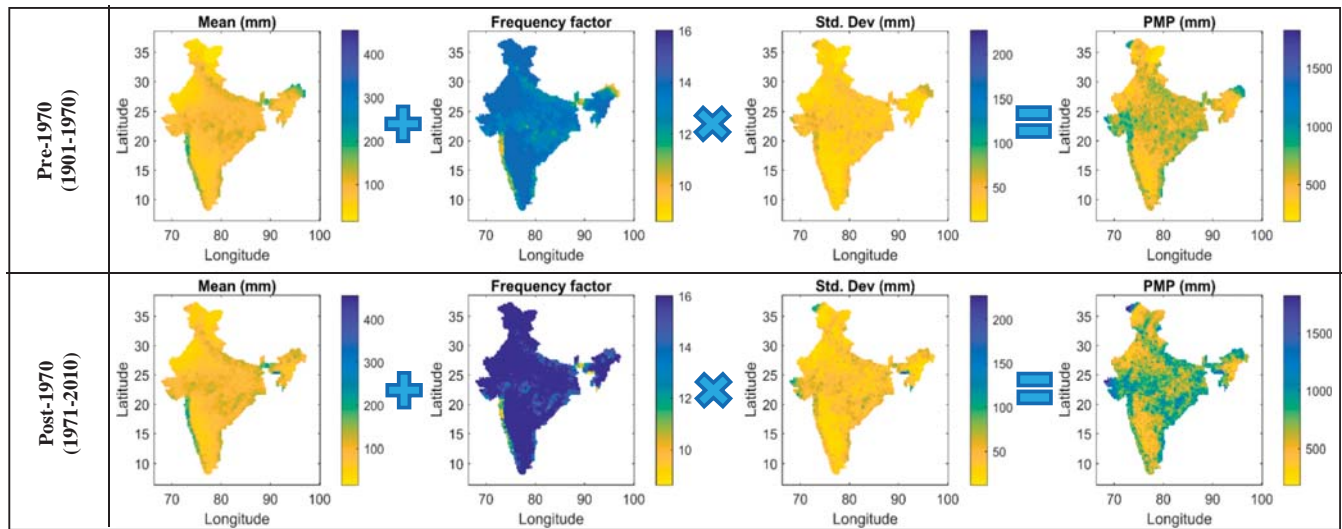


Fig. 6. Estimation of PMP using mean and standard deviation of annual daily maximum rainfall and corresponding frequency factor for two parts of historical observed data.

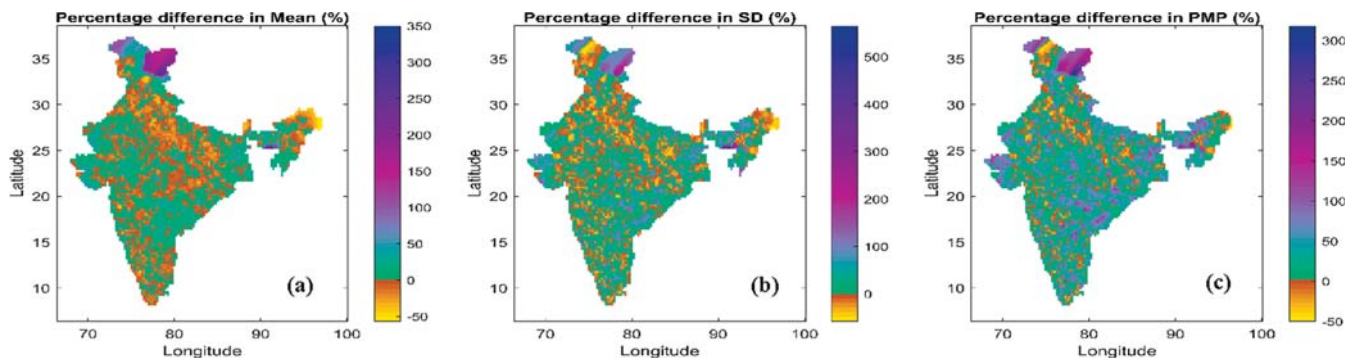


Fig. 7. Percentage difference in (a) mean and (b) standard deviation of annual daily maximum rainfall, and (c) PMP between pre-1970 and post-1970. ‘Cyan to purple’ portions in the figures show the portion of India with an increasing trend, whereas the ‘brown to yellow’ portions indicate different extents of decreasing trend in PMP. The percentage of grid-points showing increasing trend is 61.85%, 67.59% and 83.92% for mean, standard deviation and PMP, respectively. (For interpretation of the references to colour in this figure legend, the reader is referred to the web version of this article.)

Table 3a

Percentage increase in mean and standard deviation of annual maximum daily precipitation, and PMP in post-1970, compared to pre-1970.

Description	Average	Maximum	Minimum
% increase in mean	8.78	359.37	-56.93
% increase in standard deviation	24.78	565.2	-58.15
% increase in PMP	35.40	318.11	-47.38

Table 3b

Percentage area showing increase in mean and standard deviation of annual maximum daily precipitation, and PMP in post-1970 as compared to pre-1970.

Description	Quantity
% of area showing increase in mean	61.85
% of area showing increase in standard deviation	67.59
% of area showing increase in PMP	83.92

our proposed technique and Eq. (8) (as discussed in section 3.6), shown by red line in Figs. 5a and 5b. The envelope curves clearly have two different parts as discussed earlier; one straight-line, parallel to x-axis with the maximum value of K (K_m) and one exponentially decaying curve. In order to get the exponential curve, some top points from the scatter plot were selected and have been marked by orange diamond

markers in the scatter plots. However, in some cases, very few grid-points exist with unusually high values of K as compared to the other points in the study area. For example, in case of post-1970 period, few grid points (4 or 5 out of 4951) exist in west central part of India that have very high K values in range of 21–24, whereas K values mostly lie below 16 for other grid points (Fig. 5a). Now, developing the envelope curve considering those unusually high values of K will definitely lead to over estimation of PMP for remaining and most part of India. Hence, those few points are excluded while developing the upper envelope curve. However while estimating PMP for those points we have used their actual K values, not the one obtained from the envelope curve. Keeping this in mind, the envelope curves for different future time-spans across three different models are also prepared.

The equation of the exponential portion of the envelope curve is shown in the inset of these figures (Figs. 5a and 5b). Using these envelope curves (Eq. (8)), frequency factor at each grid point is re-estimated depending on the mean annual maximum daily rainfall (\bar{X}_N) at that grid point.

4.4. Development of PMP map using historical data

Using the adjusted mean and standard deviation of AMDP series, and the re-estimated frequency factor in Eq. (5), PMP is determined for each grid point in India. The spatial distribution of mean and standard deviation of AMDP, frequency factor and estimated PMP are shown in

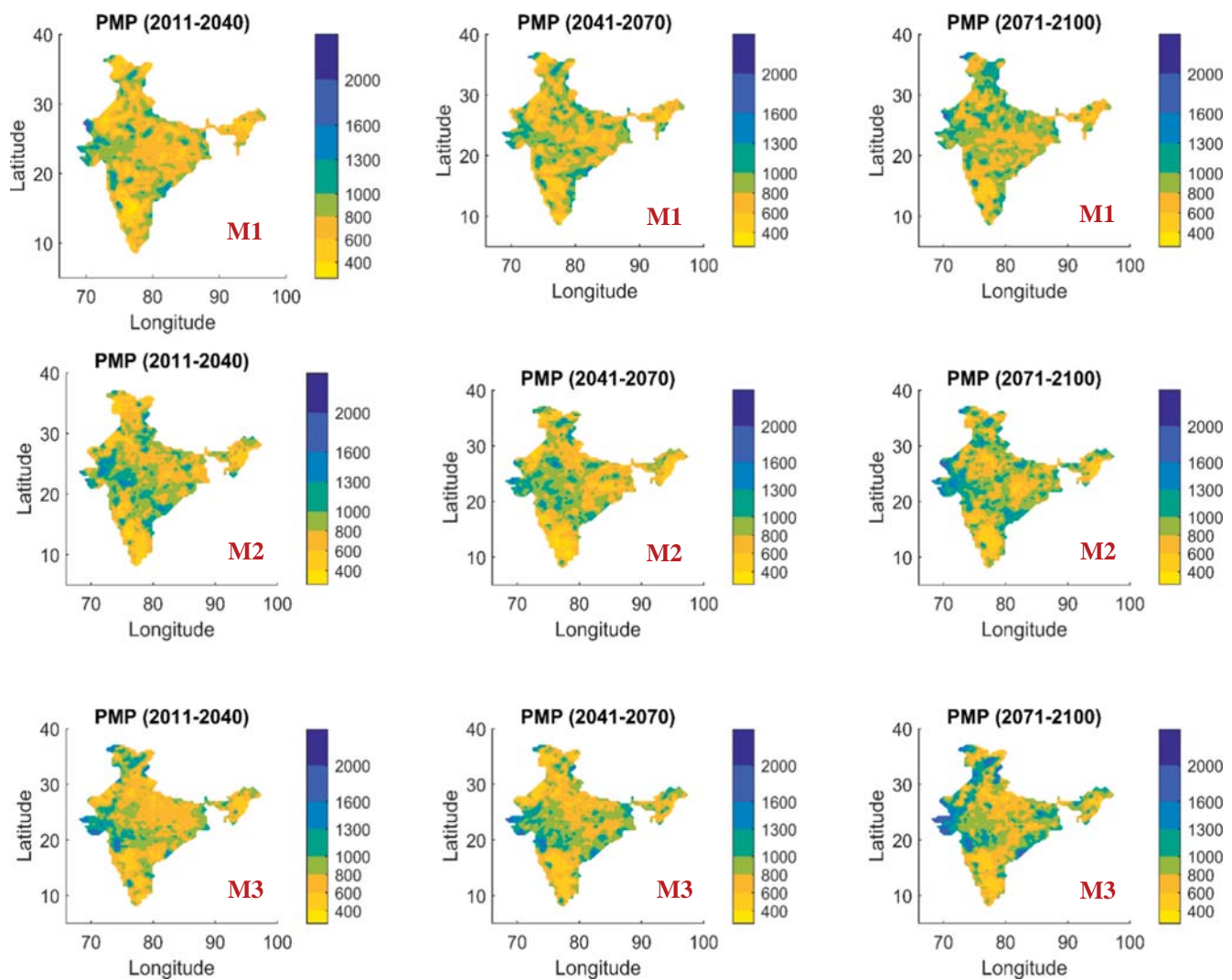


Fig. 8a. PMP map of India for three future time periods for three different models (M1, M2, and M3) used in the present study following RCP 4.5 scenario.

Fig. 6 for two parts of observed data, viz. pre-1970 and post-1970. From the maps of mean and standard deviation, in general, higher values are observed along the Western Ghats, some parts of north-east and east-central India. Comparatively lower values of mean and standard deviation are observed in the Rajasthan region, peninsular India and Kashmir portion. These basic observations match with the regular spatial variation of Indian rainfall. Finally, the estimated PMP maps for both pre-1970 and post-1970 are provided in the last column in Fig. 6. It is observed that the PMP is varying from a minimum value of 179 mm to the highest value of 1088 mm for the pre-1970 period. Whereas, for the post-1970 period estimated values of PMP is ranging between 363 mm and 1826 mm. IITM (1989) published a PMP atlas for India containing generalized charts of PMP estimates ranging from 300 mm to 1100 mm which is comparable with the pre-1970 period in the present study. Rakhecha and Clark (1999) also developed one PMP map for India based on maximisation and transposition of storm using previous 100 years data with respect to the year of analysis, which shows a PMP range of 600 mm to 1700 mm. So, the PMP estimates obtained in this study are mostly comparable with those results, at least in terms of range, which validates the applicability of Hershfield method and our proposed enveloping technique. However, the post-1970 PMP estimates are substantially higher compared to the pre-1970 estimates, as a possible consequence of climate change and global climatic shift in the 1970s.

To further investigate the extent of increase and its possible cause,

the percentage difference of mean and standard deviation of AMDP series, and the estimated PMP values in post-1970 is calculated with respect to pre-1970 at each grid-point and shown in Fig. 7a, 7b and 7c, respectively. Some basic observations from this Fig. 7 are given in quantitative terms in Tables 3a and 3b. From Fig. 7 and Table 3, it is noticed that, almost 84% area (cyan to purple portion in Fig. 7c) in India shows an increasing trend in PMP. The range of change in PMP varies from -47.38% to 318.11% . However, averaged over entire India, the percentage increase in PMP is 35.40% . Some parts of Gujarat, Rajasthan, and Meghalaya are also showing significant amount of increase in PMP. Interestingly, extreme north-east portion of India (in and around Arunachal Pradesh) shows maximum amount of reduction in PMP ($\sim 47\%$). Apart from that portion, a few other locations (around 16%) across the country exhibit a decreasing trend in PMP (brown to yellow patches in Fig. 7c).

The reason behind the overall increase in PMP is the general trend of increase in the mean and standard deviation of AMDP throughout India, which is also visually evident from Fig. 6. Moreover, compared to mean, the standard deviation is showing a higher range in percentage increase, as shown in Table 3a. On average, the increase in standard deviation is about 25%, whereas, the average increase in mean is only about 9%. Also, more grid points (67.59%) are showing an increase in standard deviation as compared to mean (61.85%), evident from Fig. 7a and 7b. This indicates that, not only the average AMDP is increasing, but also its variability (standard deviation) is increasing at a higher

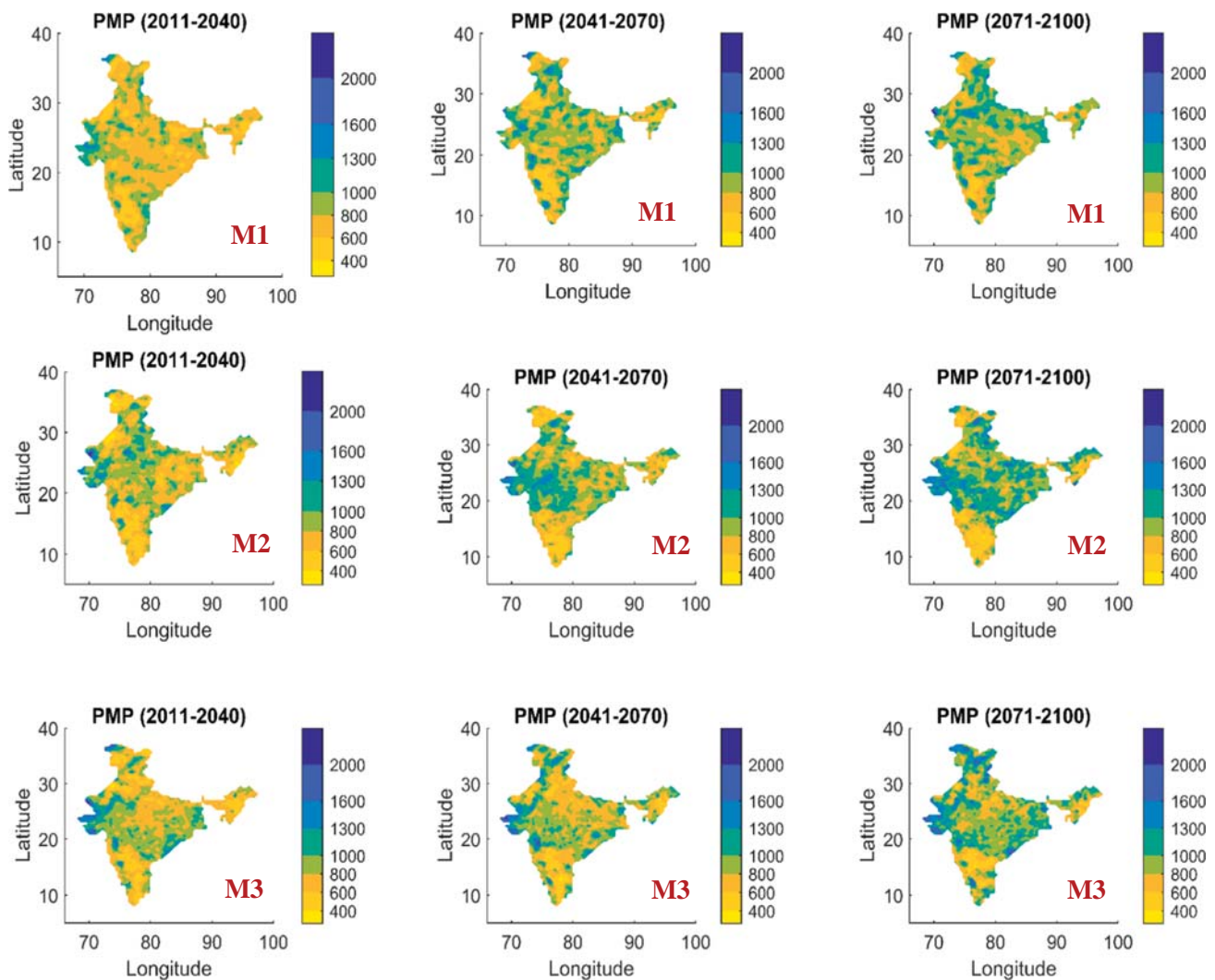


Fig. 8b. Same as Fig. 8a, but following RCP 8.5 scenario.

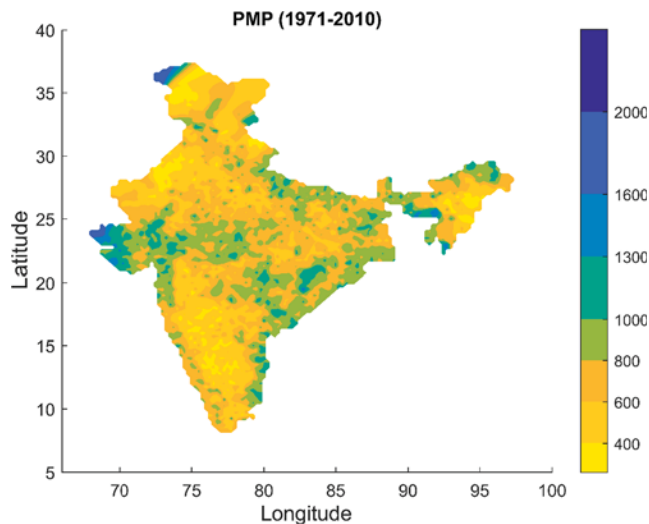


Fig. 9. PMP map developed for post-1970 period, can be used for visual comparison with Figs. 8a and 8b.

rate. As a consequence, there is a change in frequency factor, which is visually evident from Fig. 5a, which shows how considerably the scatter points (K vs. \bar{X}_N) have changed during post-1970 with respect to the

same during pre-1970. The range of K has increased; the scatter plot has become more skewed, resulting in a steeper envelope curve for K during post-1970. Therefore, an overall increase in PMP is noticed which can be considered as a significant impact of global climatic shift in the 1970s and hence of climate change (Kunkel et al., 2013; Lee et al., 2016; Chen et al., 2017; Rastogi et al., 2017). PMP is observed to increase approximately by 35% in past few decades post-1970 as compared to pre-1970. Such a level of increase can be highly detrimental for the structures designed against a stationary estimate of PMP.

4.5. PMP map using future data and comparison with recent past

The PMP maps for entire India is developed using three future projected RCM (M1, M2, and M3) data, following two scenarios (RCP 4.5 and RCP 8.5), and for three future time periods viz. near-future (2011–2040), future (2041–2070) and far-future (2071–2100). Figs. 8a and 8b show the future PMP maps developed in this study following RCP 4.5 and RCP 8.5 scenarios, respectively. Unlike the previous case of observed data, the spatial distribution of mean and standard deviation of AMDP series for future periods are not shown here for brevity. From these figures, gradual increase in PMP magnitude with the passage of time for all three models is clearly visible. Moreover, the PMP estimates are higher in the RCP 8.5 scenario, as compared to the RCP 4.5 case. Being the worst climatic projection, such observations under RCP 8.5 are quite reasonable. However, in order to visually compare these

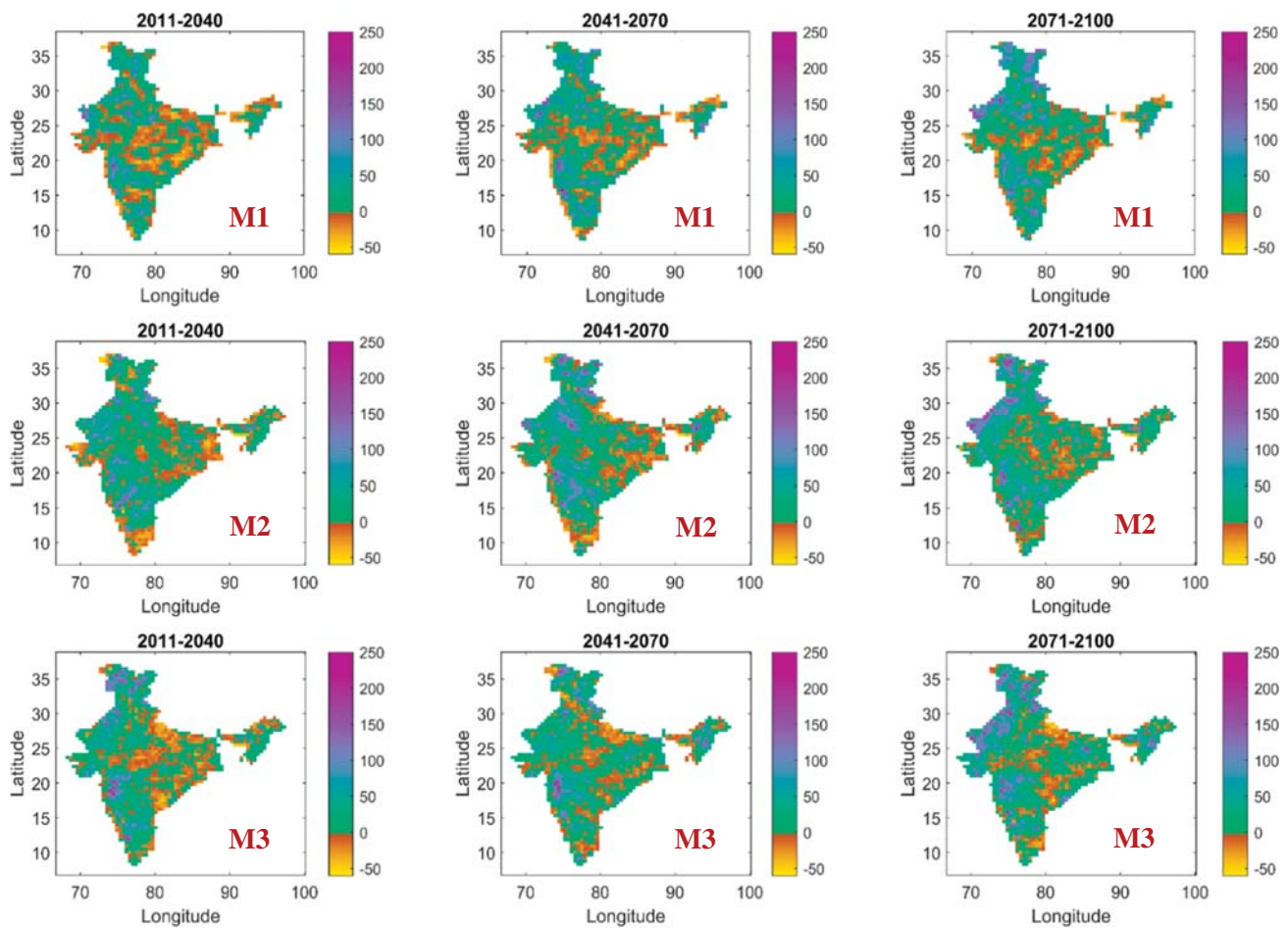


Fig. 10a. Percentage difference in PMP estimates for three future time periods for three different models (M1, M2, and M3) following RCP 4.5 scenario with respect to recent past, i.e., post-1970. ‘Cyan to purple’ portion in the figures shows the portions with an increasing trend, whereas the ‘brown to yellow’ portion indicates different extents of decreasing trend in PMP.

future PMP maps with recent past, the PMP map for post-1970 is reproduced in Fig. 9 in the same colour scale as of these future maps.

Comparing these maps from the future periods with that of the recent past, an overall increase in PMP estimates is clearly noticed throughout the country. Though the spatial distribution of future PMP varies between models, a substantial increase of PMP in west-central India, and parts of north-west India is common. Similarly, reduction in PMP estimates in the eastern and southern parts of India is also a common observation across M2 and M3. The M1 model also shows some decreasing trend of PMP in the central portion of India, though the reducing trend gradually vanishes towards the end of this century. In general, the change in PMP is captured by all three models in the future all over India. Keeping few observations of decreasing trend aside, on overall increase in PMP in most parts of India across the models is the key observation from these two figures, i.e., Figs. 8a and 8b.

Similar to observed data, in order to investigate further, some quantitative study on percentage difference in mean, standard deviation and PMP between different future time-periods and post-1970 period is performed. In order to do so, the PMP map developed for the post-1970 period with resolution $0.25^\circ \times 0.25^\circ$ is transformed to a lower resolution of $0.5^\circ \times 0.5^\circ$ (for M1) and $0.44^\circ \times 0.44^\circ$ (for M2 and M3) by IDW method, as discussed in section 3.7. The results of the comparative study for PMP are shown in Figs. 10a and 10b (percentage difference in mean and standard deviation are not shown as figure for brevity) in the form of spatial distribution throughout India. On the other hand, Table 4 shows quantitative output of this analysis i.e., average

percentage increase of PMP, and percentage of grid points showing this increment in India. Different models show different levels of increase in PMP magnitude towards the end of this century. In near-future period, this overall percentage of increase in PMP varies approximately between 7% and 16%, and in future period it ranges between 12% and 24% across different models and scenarios. Towards the end of this century, i.e. in far future period, the increment in PMP varies approximately between 20% and 28% and 29%-35% under RCP 4.5 and RCP 8.5 scenario, respectively across three models. Additionally, under both scenarios, around 70%-80% area of India shows this increasing trend across different models in far future period. Overall, a continuous increase in PMP with time is evident from the Table 4 for each model. All these observations clearly indicate towards a continuous temporal change of PMP throughout India for the rest of the present century. Reasonably similar extent of increase in PMP was also reported by Rastogi et al. (2017), where they observed around 20% increase in PMP in the 2021–2050 time period and 44% in the 2071–2100 time periods with respect to 1981–2010 baseline values in the south-eastern United States. Likewise, for Pacific Northwest (PNW) region in the USA, Chen et al. (2017) observed an increase in PMP by about $50\% \pm 30\%$ around 2099 relative to the 2016 level, following RCP 8.5. In different other parts of the world also, similar extent of increase in PMP have been reported in many studies, e.g., Lee et al. (2016) projected around 30% increase under RCP 8.5 scenario in South Korea, Afroz et al. (2015) estimated PMP to increase up to 18.2% and 27.3% in Southern Iran across different GCMs toward the end of the century w.r.t. 1971–2000 base period. Hence, though unavailability of study on future changes in

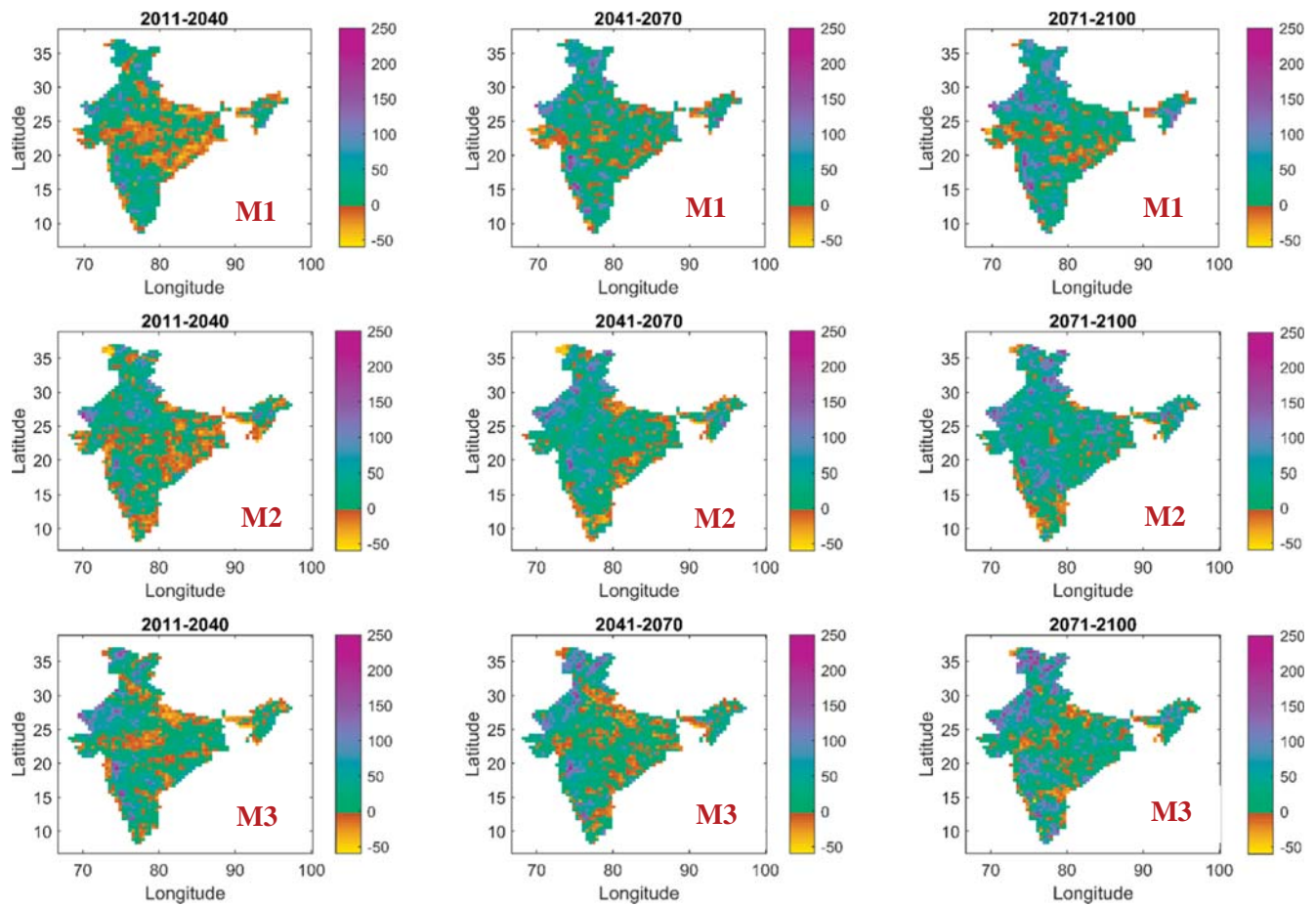


Fig. 10b. Same as Fig. 10a, but following RCP 8.5 scenario.

Table 4

Average percentage increase in PMP estimates, mean and standard deviation of AMDP series and corresponding percentage of area showing increase with respect to post-1970 period for three future time periods, following three models and two RCP scenarios.

Scenarios	Average percentage increase in PMP									Percentage of area showing increase in PMP								
	Near future (2011-2040)			Future (2041-2070)			Far future (2071-2100)			Near future (2011-2040)			Future (2041-2070)			Far future (2071-2100)		
	M-1	M-2	M-3	M-1	M-2	M-3	M-1	M-2	M-3	M-1	M-2	M-3	M-1	M-2	M-3	M-1	M-2	M-3
RCP 4.5	7.69	9.19	11.92	11.69	15.46	16.63	19.28	23.50	28.12	58.73	69.73	64.68	67.04	71.96	70.06	72.58	76.23	74.26
RCP 8.5	8.40	11.67	15.93	23.66	23.57	22.61	29.13	34.37	33.91	62.88	63.75	69.73	76.27	78.89	72.75	80.98	86.01	81.02

Scenarios	Average percentage increase in mean									Percentage of area showing increase in mean								
	Near future (2011-2040)			Future (2041-2070)			Far future (2071-2100)			Near future (2011-2040)			Future (2041-2070)			Far future (2071-2100)		
	M-1	M-2	M-3	M-1	M-2	M-3	M-1	M-2	M-3	M-1	M-2	M-3	M-1	M-2	M-3	M-1	M-2	M-3
RCP 4.5	7.62	5.74	6.34	10.00	10.64	14.56	17.72	15.87	26.31	54.66	57.58	63.16	61.86	67.63	77.87	77.10	74.85	90.22
RCP 8.5	8.39	7.59	9.30	16.53	18.41	24.32	23.69	29.80	33.74	54.11	57.12	64.21	69.62	72.95	87.72	80.05	89.88	95.67

Scenarios	Average percentage increase in standard deviation									Percentage of area showing increase in standard deviation								
	Near future (2011-2040)			Future (2041-2070)			Far future (2071-2100)			Near future (2011-2040)			Future (2041-2070)			Far future (2071-2100)		
	M-1	M-2	M-3	M-1	M-2	M-3	M-1	M-2	M-3	M-1	M-2	M-3	M-1	M-2	M-3	M-1	M-2	M-3
RCP 4.5	8.85	8.04	9.57	14.01	18.40	15.03	20.57	25.51	28.31	51.89	59.62	54.89	61.86	68.22	63.09	68.88	71.44	69.27
RCP 8.5	16.66	11.13	12.71	25.14	24.43	26.34	32.41	32.69	36.69	60.38	58.89	60.47	66.20	73.14	70.26	73.49	77.48	73.87

PMP in India limits us to compare our results to that, reasonably similar results from different other portions of the world support us to infer that, similar to different parts of the world, PMP is also expected to increase in future at a significant rate in India.

Table 4 also shows the average percentage increase and percentage of area showing that increase for mean and standard deviation along with PMP. Observing the numbers reported there, the gradual increase in mean and standard deviation with time can be identified. Also, their

spatial extent of increase increases with time. In general, we observe around 15% to 33% increase in mean in far future period under the RCP 4.5 scenario across the models, whereas the same for standard deviation is around 20% to 37%. Specifically, we observe higher extent of increase in standard deviation in most of the cases as compared to mean. So, similar to the observed data set, it can also be inferred here that, not only the mean AMDP, but their variability is also increasing (sometimes even in a faster rate), which is eventually causing a substantial increase in PMP throughout India in future.

In a nutshell, comparative study between different PMP maps developed from future simulated and observed precipitation, we can summarise that PMP estimates throughout India are showing substantial change with time. PMP was increasing in the last century and it will continue to increase over the future period too with almost similar rate. Though the projection of spatial variation and extent is different, all the models considered in this study depicts similar results. This can be considered as a possible consequence of changing climate which is intensifying the global hydrological cycle and altering the regular spatio-temporal variation of precipitation all over India (Krishnamurthy et al., 2009; Mishra and Liu, 2014; Loo et al., 2015). As a result of that, extreme rainfalls of high intensity are expected to occur in most parts of the country, causing an overall increase in mean and std. dev. in AMDP series (Ali and Mishra, 2017; Mukherjee et al., 2018), which in turn is resulting in such an extent of increase in PMP.

5. Conclusions

In this study, the likely spatio-temporal change, mostly increase, in PMP under changing climate is established across Indian mainland. Using observed records and model-simulated precipitation values, 1-day PMP maps for two different time periods from the past and three time periods from the future period are developed and compared. Future simulated precipitation values are the simulations outputs from three different GCM-RCM combinations to construct the future PMP maps under two RCP scenarios. These maps, especially the maps based on recent observations and future data, are expected to be highly informative for the hydrologists and policy makers. Following specific conclusions are drawn from the study.

- By comparing two PMP maps for historical periods, an increasing trend of PMP with an average increase of around 35% in magnitude is noticed during the post-1970 period, as compared to the pre-1970 period. It is true for the most part of India (~84% of the total area). This indicates a serious and significant impact of shift in global climate regime in the 1970s on PMP in India.
- Similar to the historical period, the increasing trends persist in the future also. All three models considered in this study show an agreement on this observation; all models show an overall increasing trend of PMP, but of different extent and spatial variation. In general, approximately 29% to 35% and 20% to 28% increase in PMP is observed in the far-future period compared to the recent past under RCP 8.5 and RCP 4.5 scenario, respectively. Also, around 70%-80% area of India shows this increasing trend across different models. This indicates that the increasing trend of PMP throughout India in the past will continue almost at a similar rate in the upcoming future period.
- Further analysis indicates that, compared to mean AMDP, the standard deviation of AMDP is increasing with a similar or even faster rate over time, and eventually resulting in the increase in the estimates of PMP with time. Apart from this, the change in frequency factor, its range and corresponding changes in the envelope curve also results in an increase in PMP.

Finally, the temporal change of PMP in India must be considered in the planning, designing and future risk assessment of any major high-risk water resources infrastructure. Any design based on the stationary

estimate of PMP is susceptible to be exposed to higher risk with the passage of time. Hence, the long-term decision-making strategies should be updated according to the future-projected PMP maps. The developed PMP maps for entire Indian mainland based on this study are available at Mendeley data repository (URL: <https://doi.org/10.17632/zx99xr4wkr.1>). For further details on the AMDP dataset used in this study and final multi-model PMP estimates for India, readers can refer to associated 'Data in Brief' article (Sarkar and Maity, 2020).

CRediT authorship contribution statement

Subharthi Sarkar: Methodology, Investigation, Writing - original draft, Formal analysis. **Rajib Maity:** Methodology, Supervision, Funding acquisition, Conceptualization, Investigation, Writing - review & editing.

Declaration of Competing Interest

The authors declare that they have no known competing financial interests or personal relationships that could have appeared to influence the work reported in this paper.

Acknowledgements

This work is partially supported by Department of Science and Technology, Climate Change Programme (SPLICE), Government of India (Ref No. DST/CCP/CoE/79/2017(G)) through a sponsored project.

References

- Afroz, A.H., Akbari, H., Rakhshandehroo, G.R., Pourtouserkani, A., 2015. Climate change impact on probable maximum precipitation in Chenar-Rahdar River Basin. *Watershed Manage.* 36–47. <https://doi.org/10.1061/9780784479322.004>.
- Ali, H., Mishra, V., 2017. Contrasting response of rainfall extremes to increase in surface air and dewpoint temperatures at urban locations in India. *Sci. Rep.* 7, 1–15. <https://doi.org/10.1038/s41598-017-01306-1>.
- Allan, R.P., Soden, B.J., 2008. Atmospheric warming and the amplification of precipitation extremes. 1481 = 1484. *Science* (80-) 321. <https://doi.org/10.1126/science.1160787>.
- Allen, M.R., Ingram, W.J., 2002. Constraints on future changes in climate and the hydrologic cycle 419.
- Beauchamp, J., Leconte, R., Trudel, M., Brissette, F., 2013. Estimation of the summer-fall PMP and PMF of a northern watershed under a changed climate. *Water Resour. Res.* 49, 3852–3862. <https://doi.org/10.1002/wrcr.20336>.
- Bruce, J.P., Clark, R.H., 1966. Introduction to hydrometeorology.
- Chavan, S.R., Srinivas, V.V., 2017. Regionalization based envelope curves for PMP estimation by Hershfield method. *Int. J. Climatol.* 3779, 3767–3779. <https://doi.org/10.1002/joc.4951>.
- Chen, F., Liu, C., 2012. Estimation of the spatial rainfall distribution using inverse distance weighting (IDW) in the middle of Taiwan. *Paddy Water Env.* 10, 209–222. <https://doi.org/10.1007/s10333-012-0319-1>.
- Chen, J., Genio, A.D. Del, Carlson, B.E., Bosilovich, M.G., 2007. The spatiotemporal structure of twentieth-century climate variations in observations and reanalyses. Part II: Pacific pan-decadal variability. *J. Clim.* 21, 2634–2651. <https://doi.org/10.1175/2007JCLI2012.1>.
- Chen, X., Hossain, F., Leung, L.R., 2017. Probable maximum precipitation in the U.S. Pacific Northwest in a Changing climate. *Water Resour. Res.* 53, 9600–9622. <https://doi.org/10.1002/2017WR021094>.
- Chow, V.T., 1951. A general formula for hydrologic frequency analysis. *Trans. Am. Geophys. Union* 32, 231–237.
- Collier, C.G., Hardaker, P.J., 1996. Estimating probable maximum precipitation using a storm model approach. *J. Hydrol.* 183, 277–306. [https://doi.org/10.1016/0022-1694\(95\)02953-2](https://doi.org/10.1016/0022-1694(95)02953-2).
- Dai, T., Dong, W., Guo, Y., Hong, T., Ji, D., Yang, S., Tian, D., Xiaohangwen, Zhu, X.A., 2018. Understanding the Abrupt Climate Change in the Mid-1970s from a Phase-Space Transform Perspective. *J. Appl. Meteorol. Climatol.* 57, 2551–2560. <https://doi.org/10.1175/JAMC-D-17-0345.1>.
- Dash, S., Maity, R., 2019. Temporal evolution of precipitation-based climate change indices across India: contrast between pre- and post-1975 features. *Theor. Appl. Climatol.* doi: 10.1007/s00704-019-02923-8.
- De Silva, R.P., Dayawansa, N.D.K., Ratnasiri, M.D., 2007. A comparison of methods used in estimating missing rainfall data. *J. Agric. Sci.* 3, 101–108.
- Desa, M., Rakhecha, P.R., 2007. Probable maximum precipitation for 24-h duration over an equatorial region: Part 2-Johor, Malaysia. *Atmos. Res.* 84, 84–90. <https://doi.org/10.1016/j.atmosres.2006.06.005>.

- Dhar, O.N., Kulkarni, A.K., Rakhechfia, P.R., 1981. Probable maximum point rainfall estimation for the southern half of the Indian peninsula. *Proc. Natl. Acad. Sci. (Earth Planet. Sci.)* 90, 39–46.
- Eliasson, J., 1997. A statistical model for extreme precipitation. *Water Resour. Res.* 33, 449–455.
- Fernando, W.C.D.K., Wickramasuriya, S.S., 2011. The hydro-meteorological estimation of probable maximum precipitation under varying scenarios in Sri Lanka. *Int. J. Climatol.* 31, 668–676. <https://doi.org/10.1002/joc.2096>.
- Giorgi, F., Coppola, E., Diffenbaugh, N.S., Gao, X.J., Marotti, L., Shi, Y., 2011. Higher hydroclimatic intensity with global warming. *J. Clim.* 24, 5309–5324. <https://doi.org/10.1175/2011JCLI3979.1>.
- Hansen, E.M., Schwarz, F.K., Riedel, J.T., 1977. Probable Maximum Precipitation Estimates, Colorado River and Great Basin Drainages. Silver Spring, MD.
- Hart, T.L., 1981. Survey of Probable Maximum Precipitation Studies using the Synoptic Method of Storm Transposition and Maximisation, in: *Proc. Workshop on Spillway Design*. AGPS Canberra, Monash University, Melbourne, pp. 53–63.
- Hershfield, D.M., 1965. Method for estimating probable maximum precipitation. *J. Am. Waterworks Assoc.* 57, 965–972.
- Hershfield, D.M., 1961. Estimating the probable maximum precipitation. *J. Div. Am. Soc. Civ. Eng.* 87, 1961.
- IITM, 1989. Probable Maximum Precipitation Atlas, Indian Institute of Tropical Meteorology.
- Jacob, D., Hagemann, S., 2007. Intensification of the hydrological cycle – an important signal of climate change 170–173.
- Jacques-coper, M., Garreaud, R.D., 2015. Characterization of the 1970s climate shift in South America 2179, 2164–2179. doi: 10.1002/joc.4120.
- Jang, S., Kavvas, M.L., 2015. Downscaling global climate simulations to regional scales: statistical downscaling versus dynamical downscaling. *J. Hydrol. Eng.* 20, 1–18. [https://doi.org/10.1061/\(ASCE\)JHE.1943-5584.0000939](https://doi.org/10.1061/(ASCE)JHE.1943-5584.0000939).
- Kendall, M., Stuart, A., 1976. *The Advanced Theory of Statistics*. Charles Griffin & Co., Ltd., London.
- Kim, N.W., Lee, J., 2016. Estimation of time-variant probable maximum precipitation for South Korea. *KSCE J. Civ. Eng.* 21, 1031–1038. <https://doi.org/10.1007/s12205-016-1052-x>.
- Klein, I.M., Rousseau, A.N., Frigon, A., Freudiger, D., Gagnon, P., 2016. Evaluation of probable maximum snow accumulation: development of a methodology for climate change studies. *J. Hydrol.* 537, 74–85. <https://doi.org/10.1016/j.jhydrol.2016.03.031>.
- Krishnamurthy, C.K.B., Lall, U., Kwon, H.-H., 2009. Changing frequency and intensity of rainfall extremes over India from 1951 to 2003. *J. Clim.* 22, 4737–4746. <https://doi.org/10.1175/2009JCLI2896.1>.
- Kulkarni, B.D., 2000. On some climatological and hydrometeorological aspects of Godavari basin for the optimum development of its water resources projects.
- Kunkel, K.E., Karl, T.R., Easterling, D.R., Redmond, K., Young, J., Yin, X., Hennon, P., 2013. Probable maximum precipitation and climate change. *Geophys. Res. Lett.* 40, 1402–1408. <https://doi.org/10.1002/grl.50334>.
- Lee, O., Park, Y., Kim, E.S., Kim, S., 2016. Projection of Korean probable maximum precipitation under future climate change scenarios. *Adv. Meteorol.* 2016, 1–16. <https://doi.org/10.1155/2016/3818236>.
- Loo, Y.Y., Billa, L., Singh, A., 2015. Effect of climate change on seasonal monsoon in Asia and its impact on the variability of monsoon rainfall in Southeast Asia. *Geosci. Front.* 6, 817–823. <https://doi.org/10.1016/j.gsf.2014.02.009>.
- Madakumbura, G.D., Kim, H., Utsumi, N., Shioyama, H., Fischer, E.M., Seland, Ø., Scinocca, J.F., Mitchell, D.M., 2019. Event-to-event intensification of the hydrologic cycle from 1.5 °C to a 2 °C warmer world 1–7. doi: 10.1038/s41598-019-39936-2.
- Maity, R., 2018. *Statistical Methods in Hydrology and Hydroclimatology*, first ed. Springer, Singapore.
- Maity, R., Suman, M., Laux, P., Kunstmann, H., 2019. Bias correction of zero-inflated RCM precipitation fields: a copula-based scheme for both mean and extreme conditions. *J. Hydrometeorol.* 595–611. <https://doi.org/10.1175/JHM-D-18-0126.1>.
- Mazumder, K.C., Rangarajan, R., 1966. Regional storm analysis. *Mazumder, Indian J. Meteorol. Geophys.* 17, 1966.
- Meehl, G.A., Hu, A., Santer, B.D., 2008. The mid-1970s climate shift in the Pacific and the relative roles of forced versus inherent decadal variability. *J. Clim.* 22, 780–792. <https://doi.org/10.1175/2008JCLI2552.1>.
- Milly, P.C.D., Betancourt, J., Falkenmark, M., Hirsch, R.M., Kundzewicz, Z.W., Lettenmaier, D.P., Stouffer, R.J., 2008. Stationarity is dead: whither water management? *Science* (80-) 319, 573–574. <https://doi.org/10.1126/science.1151915>.
- Mishra, A., Liu, S.C., 2014. *Journal of Geophysical Research: Atmospheres*. *J. Geophys. Res. Atmos.* 119, 7833–7841. doi: 10.1002/2014JD021471. Received.
- Mukherjee, S., Aadhar, S., Stone, D., Mishra, V., 2018. Increase in extreme precipitation events under anthropogenic warming in India. *Weather Clim. Extrem.* 20, 45–53. <https://doi.org/10.1016/j.wace.2018.03.005>.
- Myers, V.A., 1967. Meteorological estimation of extreme precipitation for spillway design floods. *Weather bur. Tech. Memo. Wbmn hydro 5*, 1–31.
- Nelsen, R.B., 2006. *An Introduction to Copulas*, second ed. Springer, New York.
- Nikulin, G., Kjellström, E., Hansson, U.L.F., Strandberg, G., Ullerstig, A., 2011. Evaluation and future projections of temperature, precipitation and wind extremes over Europe in an ensemble of regional climate simulations. *Tellus* 63A, 41–55. <https://doi.org/10.1111/j.1600-0870.2010.00466.x>.
- NRLD, 2018. National Register of Large Dams, available at: <http://www.indiaenvironmentportal.org.in/files/file/NRLD%202018.pdf>, Accessed on February, 2019.
- O’Gorman, P.A., 2015. Precipitation extremes under climate change. *Curr. Clim. Chang. Rep.* 49–59. <https://doi.org/10.1007/s40641-015-0009-3>.
- Prasad, R., Hibler, L.F., Coleman, A.M., Ward, D.L., 2011. Design-Basis Flood Estimation for Site Characterization at Nuclear Power Plants in the United States of America. Richland, WA 99352.
- Rakhecha, P.R., Clark, C., 1999. Revised estimates of one-day probable maximum precipitation (PMP) for India. *Meteorol. Appl.* 6, 343–350. <https://doi.org/10.1017/S1350482799001280>.
- Rakhecha, P.R., Deshpande, N.R., Soman, M.K., 1992. Probable maximum precipitation for a 2-day duration over the Indian Peninsula. *Theor. Appl. Climatol.* 45, 277–283. <https://doi.org/10.1007/BF00865518>.
- Ramak, Z., Porhemmat, J., Sedghi, H., Fattahi, E., Lashni-Zand, M., 2017. The climate change effect on probable maximum precipitation in a catchment. A case study of the Karun river catchment in the Shalu bridge site (Iran). *Russ. Meteorol. Hydrol.* 42, 204–211. <https://doi.org/10.3103/S1068373917030086>.
- Rastogi, D., Kao, S.-C., Ashfaq, M., Mei, R., Kabela, E.D., Gangrade, S., Naz, B.S., Preston, B.L., Singh, N., Anantharaj, V.G., 2017. Effects of climate change on probable maximum precipitation: A sensitivity study over the Alabama-Coosa-Tallapoosa River Basin. *J. Geophys. Res. Atmos.* 122, 4808–4828.
- Rouhani, H., Leconte, R., 2016. A novel method to estimate the maximization ratio of the Probable Maximum Precipitation (PMP) using regional climate model output. *Water Resour. Res.* 52, 7347–7365. <https://doi.org/10.1002/2016WR018977>. Received.
- Rousseau, A.N., Klein, I.M., Freudiger, D., Gagnon, P., Frigon, A., Ratté-Fortin, C., 2014. Development of a methodology to evaluate probable maximum precipitation (PMP) under changing climate conditions: application to southern Quebec, Canada. *J. Hydrol.* 519, 3094–3109. <https://doi.org/10.1016/j.jhydrol.2014.10.053>.
- Sabeerali, C.T., Rao, S.A., Ajayamohan, R.S., Murtugudde, R., 2012. On the relationship between Indian summer monsoon withdrawal and Indo-Pacific SST anomalies before and after 1976/1977 climate shift. *Clim. Dyn.* 39, 841–859. <https://doi.org/10.1007/s00382-011-1269-9>.
- Sarkar, S., Maity, R., 2020. High-resolution One-day Probable Maximum Precipitation dataset across India and its Future-projected changes over India. Data in Brief. Elsevier <https://doi.org/10.1016/j.dib.2020.105525>. In press.
- Schreiner, L.C., Riedel, J.T., 1978. Probable maximum precipitation estimates, United States east of the 105th meridian. Silver Spring, MD.
- Sharma, P.B., Nathan, K.K., Rao, G., 1975. Analysis of maximum precipitation over coastal Andhra Pradesh, in: *Proceedings of Second World Congress. International Water Resources Association, New Delhi*, pp. 471–487.
- Singh, A., Singh, V.P., Byrd, A.R., 2018. Computation of probable maximum precipitation and its uncertainty. *Int. J. Hydrol.* 2 (4), 504–514. <https://doi.org/10.15406/ijh.2018.02.00118>.
- Stratz, S.A., Hossain, F., 2014. Probable maximum precipitation in a changing climate: implications for dam design. *J. Hydrol. Eng.* 19, 6014006. [https://doi.org/10.1061/\(ASCE\)JHE.1943-5584.0001021](https://doi.org/10.1061/(ASCE)JHE.1943-5584.0001021).
- Tang, W.Y., Kassim, A.H.M., Abubakar, S.H., 1996. Comparative studies of various missing data treatment methods Malaysian experience. *Atmos. Res.* 42, 247–262.
- Thuy, T.T., Le, Kawagoe, S., Sarukkalgie, R., 2019. Regional studies estimation of probable maximum precipitation at three provinces in Northeast Vietnam using historical data and future climate change scenarios. *J. Hydrol. Reg. Stud.* 23, 100599. <https://doi.org/10.1016/j.ejrh.2019.100599>.
- Trenberth, K.E., Dai, A., Rasmussen, R.M., Parsons, D.B., 2003. The changing character of precipitation. *Bull. Am. Meteor. Soc.* 84, 1205–1217. <https://doi.org/10.1175/BAMS-84-9-1205>.
- Utsumi, N., Seto, S., Kanae, S., Maeda, E.E., Oki, T., 2011. Does higher surface temperature intensify extreme precipitation? *Geophys. Res. Lett.* 38, 1–5. <https://doi.org/10.1029/2011GL048426>.
- Wang, H., 2001. The weakening of the Asian monsoon circulation after the end of 1970’s. *Adv. Atmos. Sci.* 18, 376–386. <https://doi.org/10.1007/BF02919316>.
- Wang, B., Wu, R., Lau, K.-M., 2001. Interannual variability of the Asian summer monsoon: contrasts between the Indian and the Western North Pacific – East Asian Monsoons. *J. Clim.* 14, 4073–4090.
- Wiesner, C.J., 1970. *Hydrometeorology*. Chapman and Hall Ltd., London.
- WMO, 1966. *Climate Change*. World Meteorological Organisation, WMO Tech note, vol. 79. Geneva, 79.
- WMO, 1986. *Manual for estimation of probable maximum precipitation*, World Meteorological Organisation, Operational Hydrology Report No.1, Second Edition, WMO No. 332.
- WMO, 2009. *Manual on estimation of probable maximum precipitation*, World Meteorological Organisation (WMO No. 1045), available at: <http://www.wmo.int/pages/prog/hwrr/publications/PMP/WMO%201045%20en.pdf>, Accessed on February, 2019.
- Xia, Y., Fabian, P., Stohl, A., Winterhalter, M., 1999. Forest climatology: estimation of missing values for Bavaria, Germany. *Agric. For. Meteorol.* 96, 131–144.
- Zhou, T., Yu, R., Zhang, J., Drange, H., Cassou, C., Deser, C., Hodson, D.L.R., Sanchez-Gomez, E., Li, J., Keenlyside, N., Xin, X., Okumura, Y., 2009. Why the Western Pacific Subtropical High Has Extended Westward since the Late 1970s. *J. Clim.* 22, 2199–2215. <https://doi.org/10.1175/2008JCLI2527.1>.